ISSN 0036-0236, Russian Journal of Inorganic Chemistry, 2008, Vol. 53, No. 2, pp. 157–163. © Pleiades Publishing, Inc., 2008.
Original Russian Text © S.A. Solopan, A.G. Belous, O.I. V'yunov, L.L. Kovalenko, 2008, published in Zhurnal Neorganicheskoi Khimii, 2008, Vol. 53, No. 2, pp. 197–203.

HIGH-TEMPERATURE SUPERCONDUCTORS

$BaTi_{1-x}Sn_xO_3$ Solid Solutions: Solid-Phase and Sol–Gel Syntheses and Characterization

S. A. Solopan, A. G. Belous, O. I. V'yunov, and L. L. Kovalenko

Vernadskii Institute of General and Inorganic Chemistry, National Academy of Sciences of Ukraine, Kiev, Ukraine

Received July 20, 2006

Abstract—$Ba(Ti_{1-x}Sn_x)O_3$solid solutions were synthesized by the sol–gel process and solid-phase reactions, and their electrophysical properties studied. $SnCl_4 \cdot 5H_2O$, $TiCl_4$, and $BaCO_3$ were precursors in the sol–gel process. IR spectroscopy, X-ray powder diffraction, and differential thermal analysis were used to study the formation conditions for $BaTiO_3$, $BaSnO_3$, and $BaTi_{0.85}Sn_{0.15}O_3$.

DOI: 10.1134/S0036023608020010

Barium titanates and barium stannate solid solutions are widely used for manufacturing various materials [1–5]. The solid-phase synthesis of $BaTi_{1-x}Sn_xO_3$ solid solutions usually proceeds from TiO_2, SnO_2, and $BaCO_3$. In this case, a single-phase product is generated at high heat-treatment temperatures: 1360–1400°C [6, 7]. The feasibility of preparing these materials at lower temperatures has been recently demonstrated using the sol–gel process, in particular, Pechini's complex polymerization process [8–11]. Metal alkoxides $[Ti(OC_4H_9\text{-}n)_4]$, $[Ti(OC_3H_7\text{-}i)_4]$, $[Sn(OC_3H_7\text{-}i)_4]$, and $[Sn(CH_3COO)_4]$ are, as a rule, used in this process [12, 13]; these reagents present a few problems (the requirement of an inert atmosphere during the entire synthesis, high costs, and difficult preparation of the reagents because of their moisture sensitivity), and it is difficult to obtain single-phase products. The use of chlorides ($SnCl_4 \cdot 5H_2O$ and $TiCl_4$) avoids these problems, and makes it possible to carry out experiments with larger amounts of reagents and to use an inert atmosphere only at the first stage (to dissolve titanium chloride in alcohol).

This work studies the parameters of the sol–gel process for the synthesis of barium titanate, barium stannate, and their solid solutions proceeding from $SnCl_4 \cdot 5H_2O$, $TiCl_4$, and $BaCO_3$.

EXPERIMENTAL

$Ba(Ti_{1-x}Sn_x)O_3$ solid solutions were prepared by the sol–gel process [11] using the scheme as shown in Fig. 1 and by solid-phase reactions.

The sol–gel synthesis of fine-grained powders was carried out as follows. Titanium chloride (high purity grade, 0.1 mol) was dissolved in isopropanol (pure for analysis C_3H_7OH, PrOH) under a dry argon atmosphere; to the resulting yellow solution, anhydrous citric acid (pure for analysis $C_6H_8O_7$, CA; 1 mol) was added; and the mixture was heated at 80 ± 5°C in air until the acid completely dissolved. Then, ethylene glycol (pure for analysis $C_2H_6O_2$, EG; 4 mol) was poured, followed by addition of the required amount of $SnCl_4 \cdot 5H_2O$ (chemically pure grade) dissolved in isopropanol and anhydrous $BaCO_3$ (chemically pure grade, 0.1 mol). The resulting solution was stirred and heated in air at 135 ± 5°C until a yellow viscous polymeric gel appeared. The gel was gradually heated to 350 ± 10°C; it polymerized to a resinous mass. Gel pyrolysis occurred at 350 ± 10°C (3 h). The product was stirred and calcined in an Al_2O_3 crucible under an air atmosphere at 1000°C for 4 h.

The reagents used for solid-phase reactions [6, 7] were $BaCO_3$, TiO_2, and SnO_2, all of high purity grade. Stoichiometric amounts of the dried reagents were blended and homogenized by corundum milling bodies for 8 h with bidistilled water. The resulting feedstock was dried, stirred, and heat-treated at 1100°C for 4 h.

The single-phase products of the sol–gel process or solid-phase reactions were triturated with aqueous polyvinyl alcohol and compacted to disks. Ceramics were sintered at temperatures in the range 1300–1400°C for 1 h.

Thermogravimetric studies were carried out on a Q-1000 OD-102 derivatograph; the heating rate was 10 K/min. The phase composition of products was determined from their powder X-ray diffraction patterns, which were recorded on a DRON 4-07 diffractometer (CuK_α radiation). The unit cell parameters and atomic coordinates for single-phase products were refined using the Rietveld technique. IR spectra in the range 400–2000 cm^{-1} were recorded as potassium bromide disks on a Specord M30 spectrometer.

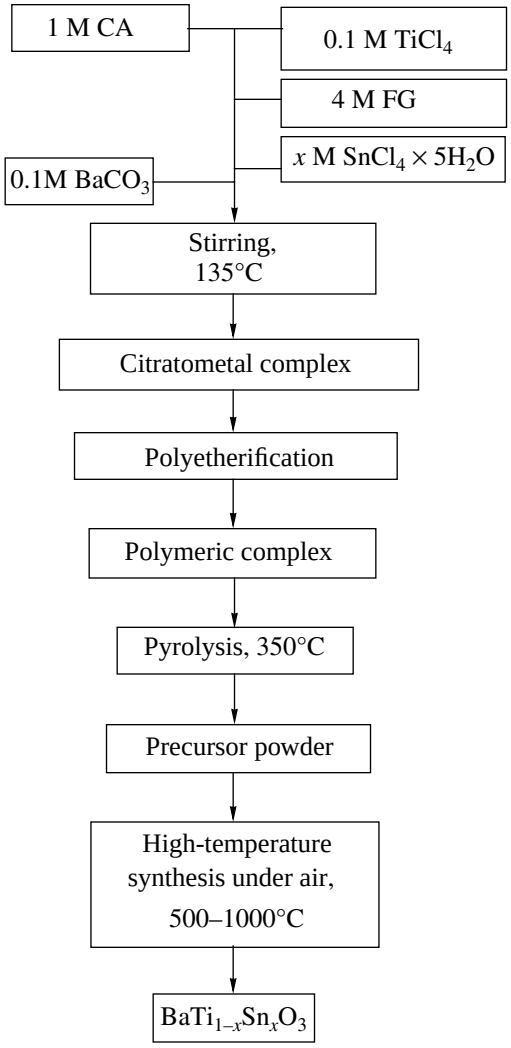

Fig. 1. Scheme of the sol–gel process for $BaTi_{1-x}Sn_xO_3$ synthesis.

The particle sizes of powders and the grain sizes of ceramics were determined on JEOL JSM-T20 and Superprobe 733 electron microscopes.

Electrophysical properties were measured over wide a frequancy range on a VM-560 Q-meter. 4

RESULTS AND DISCUSSION

Studies of the sol–gel synthesis of barium titanate, barium stannate, and their solid solutions showed that, 3 in all cases, a single-phase product was produced by the same mechanism.

According to the scheme of $BaTi_{1-x}Sn_xO_3$ synthesis (Fig. 1), titanium chloride dissolution in isopropanol yields substituted titanium alkoxide [14, 15]:

$$TiCl_4 + Pr^iOH \longrightarrow TiCl_2(O^iPr)_2 + HCl. \quad (1)$$

Addition of ethylene glycol clarifies the solution, which signifies the generation of a stable complex according to reaction (2) and in agreement with data in [16].

$$TiCl_2(O^iPr)_2 + 4HO{-}CH_2CH_2{-}OH \longrightarrow \longrightarrow Ti(OC_2H_4OH)_4 \cdot Pr^iOH + 2HCl + Pr^iOH. \quad (2)$$

When tin chloride is added to the resulting solution (which contains an excess of isopropanol and ethylene glycol), the reactions are as reactions (1) and (2) for titanium [17, 19]. When barium carbonate is added, carbon dioxide is expelled, signifying the formation of a barium complex with citric acid in agreement with [20]:

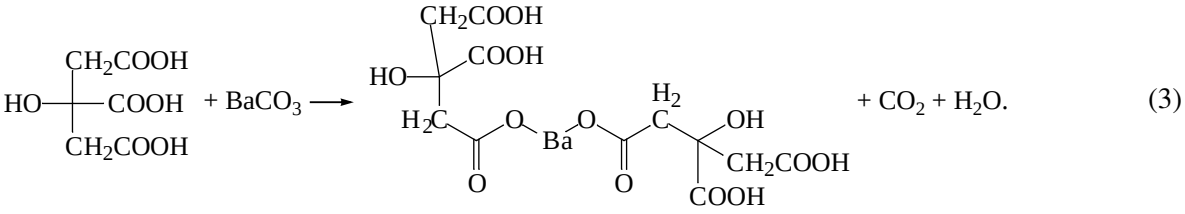

(3)

Stirring and heating the mixture to 135°C induces 2 polyetherification of citrato complexes and ethylene glycol by reaction (4), signified by the appearance of a light yellow gel and the disappearance of the ethylene glycol smell, which also agrees with the literature [11]. A rise in temperature to 350°C induces gel pyrolysis.

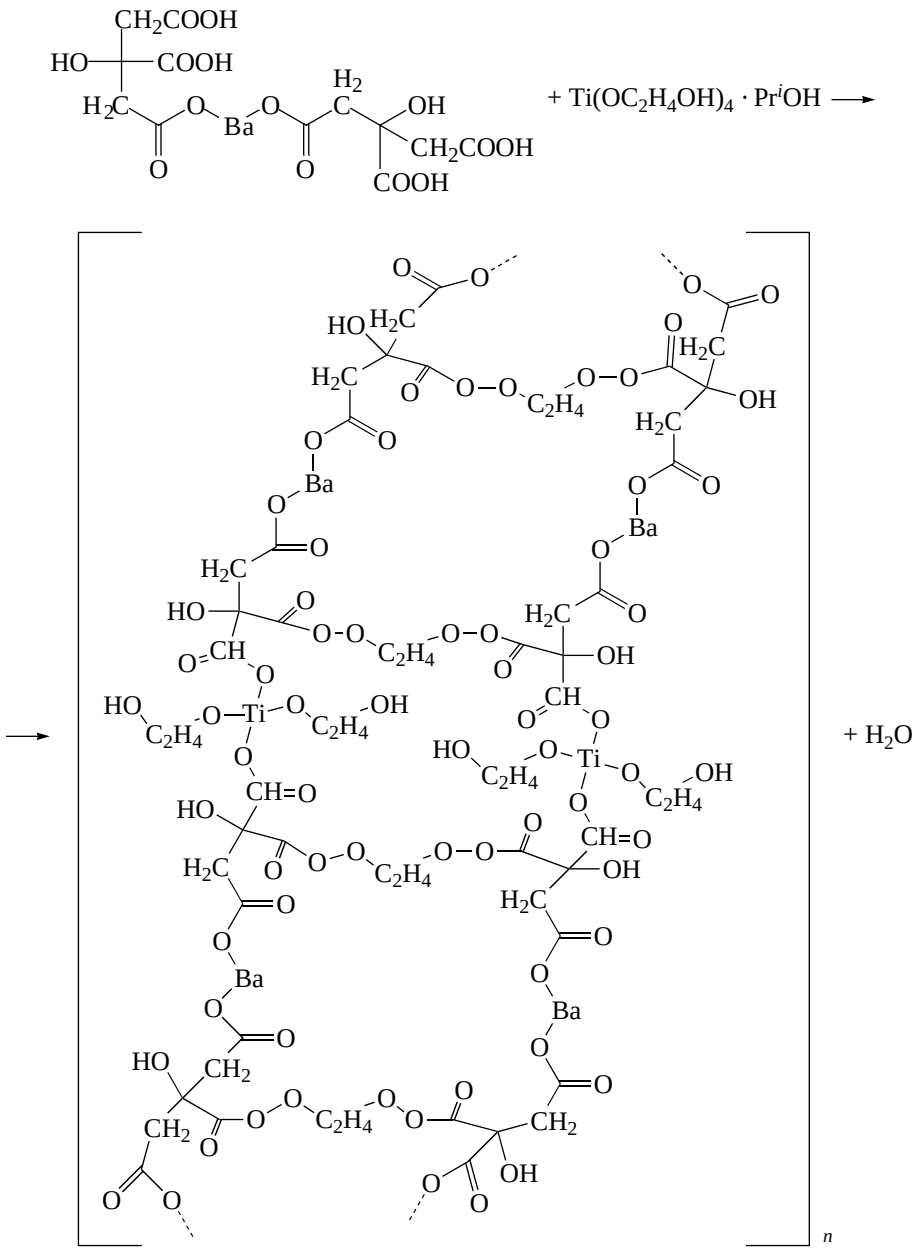

(4)

Figure 2 shows thermal curves for the precursor used to prepare a $BaTi_{0.85}Sn_{0.15}O_3$ sample. There are three weight-loss regions on the TG curve: 20–150, 250–500, and 500–750°C. The weight loss in the range 20–200°C indicates the loss of sorbate water from the gel.

The weight loss in the range 250–600°C is accompanied by a strong exotherm at 400°C. The product of heat treatment at 400°C is amorphous to X-rays (Fig. 3). In the IR spectra (Fig. 4), however, there are absorption bands at 1430 and 860 cm^{-1} due to, respectively, the stretching and bending vibrations of carbonate groups [21]. We may, therefore, infer that the exotherm at 400°C is associated with barium carbonate formation.

The insignificant weight loss (Fig. 2) in the range 500–750°C is associated with barium carbonate

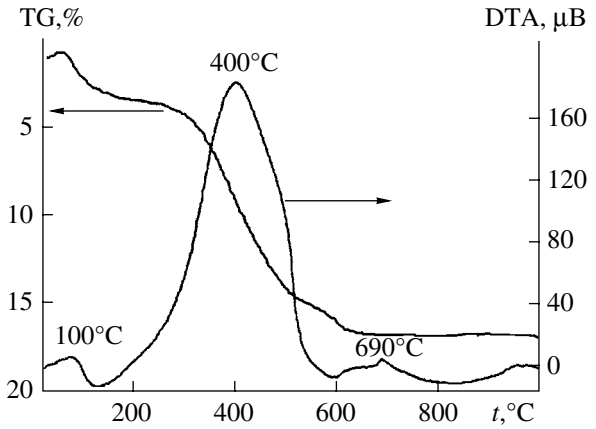

Fig. 2. Thermoanalytical curves for the precursor used to prepare a $BaTi_{0.85}Sn_{0.15}O_3$ sample.

decomposition. The exotherm at ~700°C indicates the onset of formation of solid solution $BaTi_{0.85}Sn_{0.15}O_3$. When the heat-treatment temperature rises to 800°C, reflections from $BaTi_{1-x}Sn_xO_3$ appear in the X-ray diffraction pattern together with $BaCO_3$ and TiO_2 reflections (Fig. 3). In the IR spectra (Fig. 4), absorption intensities at 1430 and 860 cm^{-1} decrease; a further rise in heat-treatment temperature makes them disappear. Single-phase $BaTi_{1-x}Sn_xO_3$ is formed after heat treatment at1000°C as shown by X-ray powder diffraction and IR spectra.

Particle sizes of powders were determined from electron-microscopic studies (Fig. 5a). The results of these studies show that all powders synthesized are nanosized: particle sizes for all samples are 40–60 nm.

The X-ray diffraction patterns of single-phase samples were used to refine the unit cell parameters and atomic coordinates (Fig. 6). The unit cell parameters calculated for $BaTi_{1-x}Sn_xO_3$ samples prepared by various processes are listed in the table [22, 23]. The samples prepared by the sol–gel process have larger unit cell parameters than those of the samples prepared by solid-phase reactions. This fact can be explained by the production of nanoparticles, whose sintering generates surface defects in ceramics. Nanoparticle production is also indicated by X-ray diffraction peak broadening (Fig. 6).

Sintering of nanopowders generates coarse-grained ceramics with grain sizes up to 20 μm (Fig. 5b). Finer grains with sizes up to 1 μm are also observed in micrographs; their existence increases the surface defect density.

Figure 7 shows the dielectric constant and dielectric loss tangent as functions of temperature for solid-phase and sol–gel samples. For the sol–gel samples, the dielectric constants are higher than for samples prepared by the solid-phase process. In the $BaTi_{0.85}Sn_{0.15}O_3$ sample prepared by the sol–gel process, in addition, dielectric loss increases, which can

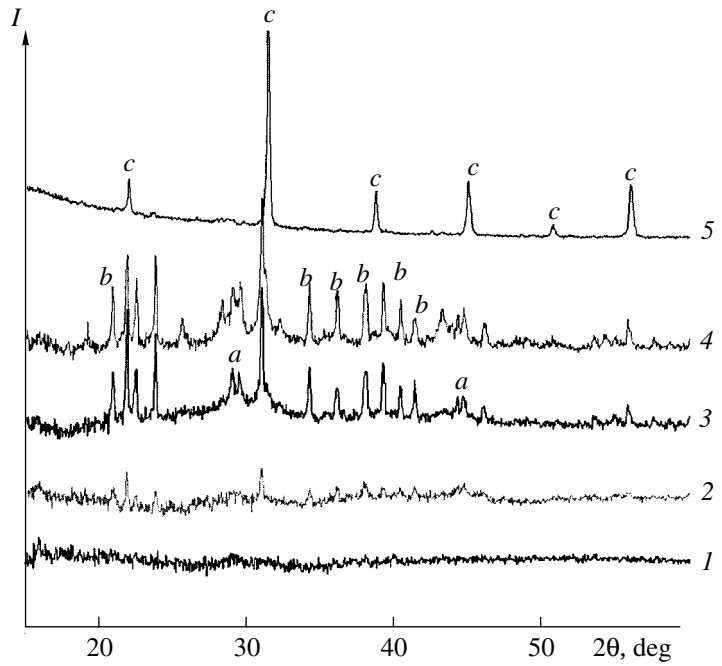

Fig. 3. X-ray diffraction patterns for the precursor used to prepare a $BaTi_{0.85}Sn_{0.15}O_3$ sample at various heat-treatment temperatures, °C: (*1*) 400, (*2*) 700, (*3*) 800, (*4*) 900, and (*5*) 1000. Notation: *a*, TiO_2; b, $BaCO_3$; and *c*, $BaTi_{0.85}Sn_{0.15}O_3$.

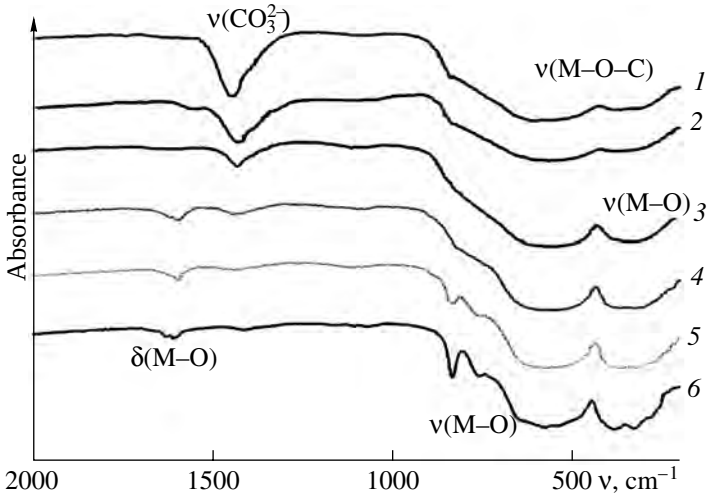

Fig. 4. IR absorption spectrum of the precursor for preparing a $BaTi_{0.85}Sn_{0.15}O_3$ sample at various heat-treatment temperatures, °C: (*1*) 350, (*2*) 600, (*3*) 700, (*4*) 800, (*5*) 900, and (*6*) 1000.

signify the appearance of stresses in the crystal structure.

Figure 8 shows the dielectric constant and dielectric loss tangent as functions of electric field strength for $BaTi_{0.85}Sn_{0.15}O_3$ samples. For the sol–gel sample, the dielectric constant varies more abruptly as a function electric field. The same is observed for the dielectric loss tangent as a function of electric field. This can be explained by stresses in the crystal structure, which are in turn associated with simultaneous formation of coarse and fine grains in the ceramics. A factor characterizing quadratic nonlinearity is used as a measure of dielectric nonlinearity: $\alpha = (1/\varepsilon)(\Delta\varepsilon/\Delta E)$ [24]. For the sol–gel sample, the nonlinearity factor is six times that for the solid-phase sample.

To summarize, we used DTA, X-ray powder diffraction, and IR spectroscopy to study the features of synthesis of nanopowders and ceramics of individual compounds $BaTiO_3$ and $BaSnO_3$ and solid solution $BaTi_{0.85}Sn_{0.15}O_3$ proceeding from $SnCl_4 \cdot 5H_2O$, $TiCl_4$, and $BaCO_3$.

Single-phase products were formed at 800°C; the products completely became a single phase after heat treatment at 1000°C.

We studied the electrophysical properties of $Ba(Ti_{1-x}Sn_x)O_3$ ceramics prepared by the sol–gel and solid-phase processes.

The sol–gel process produces nanoparticles, which are sintered to ceramics with high nonlinearity factors.

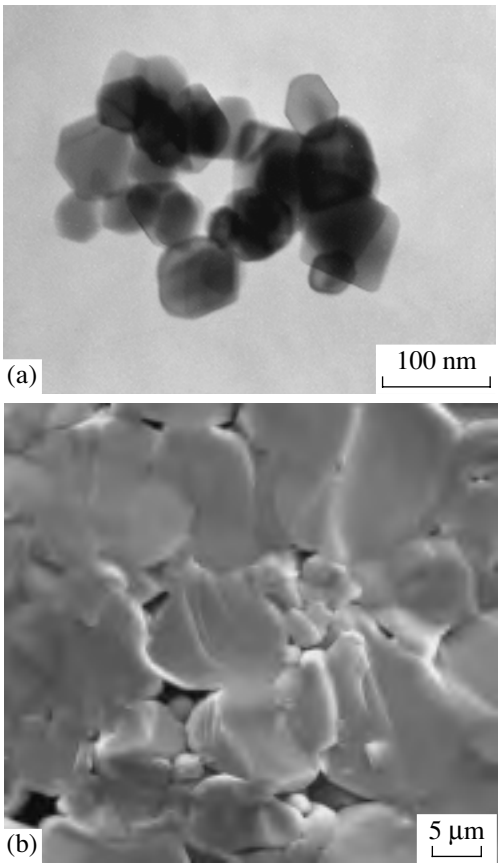

Fig. 5. Electron micrographs of (a) a $BaSnO_3$ powder prepared by the sol–gel process and (b) $BaTi_{0.85}Sn_{0.15}O_3$ ceramics.

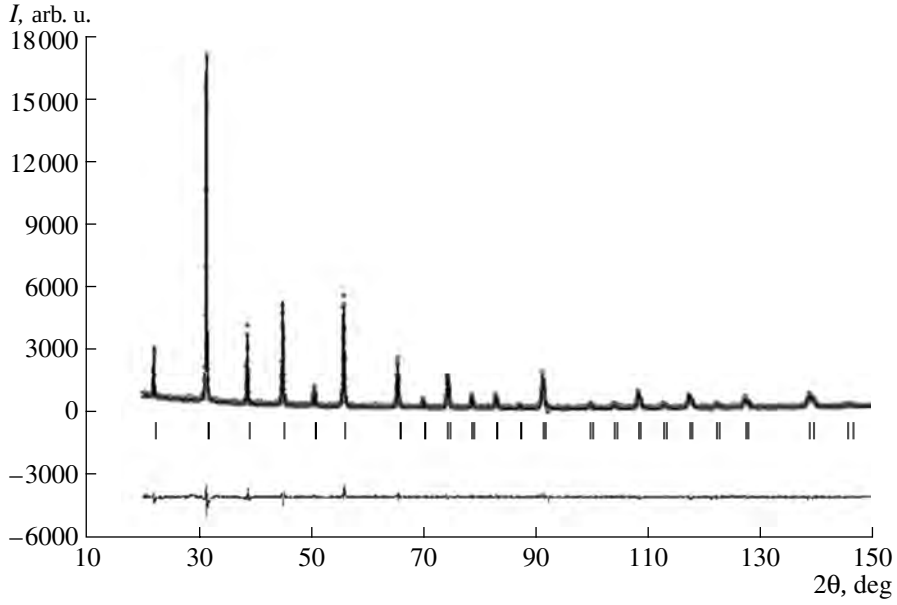

Fig. 6. X-ray diffraction pattern of a $BaTi_{0.85}Sn_{0.15}O_3$ sample after heat treatment at 1000°C and the results of full-profile analysis.

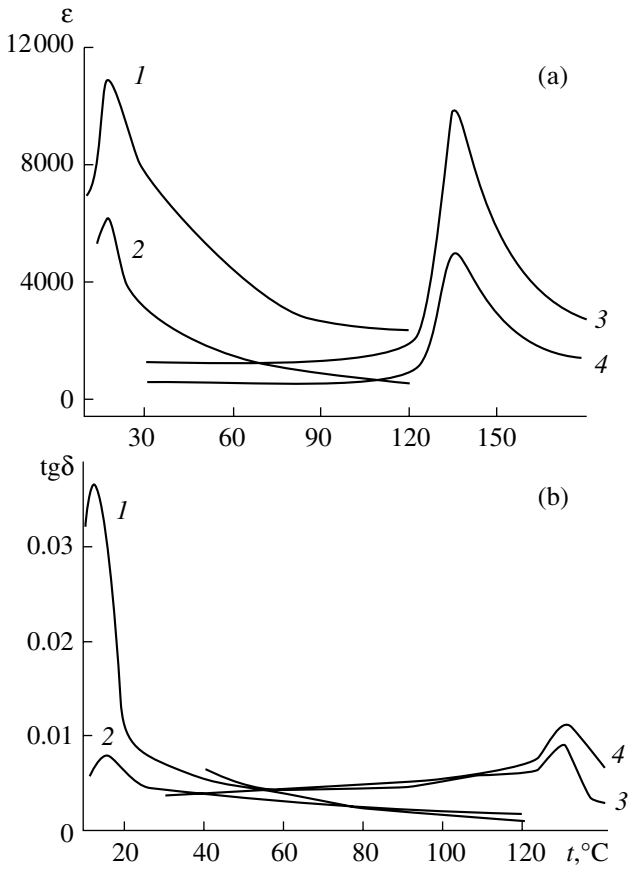

Fig. 7. (a) Dielectric constant and (b) dielectric loss tangent vs. temperature measured at 1.33 MHz for $Ba(Ti_{1-x}Sn_x)O_3$ samples with x = (*1*, *2*) 0.15 and (*3*, *4*) 0.0. Samples were prepared by (*1*, *3*) sol–gel and (*2*, *4*) solid-phase processes.

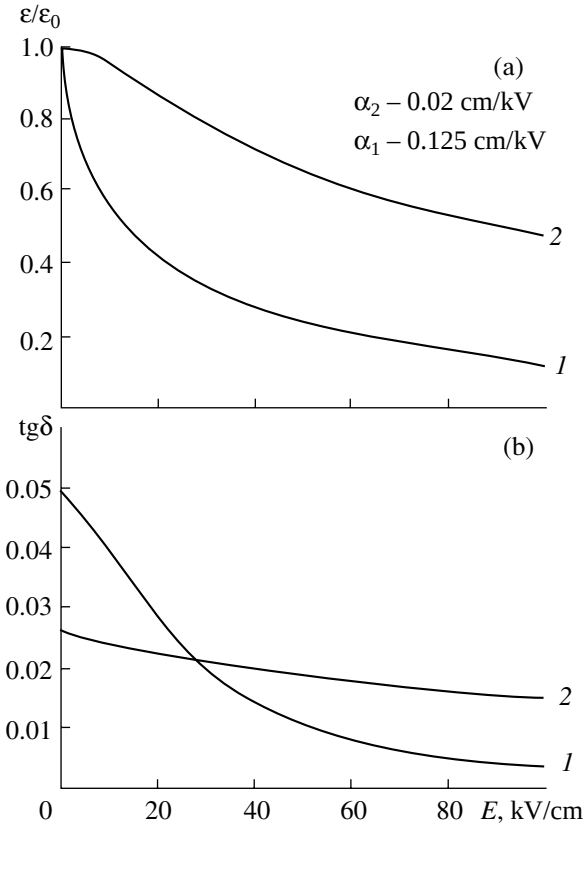

Fig. 8. (a) Dielectric constant and (b) dielectric loss tangent vs. electrical field strength measured at 1.33 MHz for a $BaTi_{0.85}Sn_{0.15}O_3$ sample prepared by (*1*, *3*) sol–gel and (*2*, *4*) solid-phase processes.

Unit cell parameters and atomic coordinates for $Ba(Ti_{1-x}Sn_x)O_3$ samples prepared by various methods

Composition	Preparation method	Space group	*a*, Å	*c*, Å	*V*, Å^3	z_{Ba}	z_{O1}	z_{O2}
$BaTiO_3$	Solid-phase	*P*4*mm*	3.994(1)	4.034(1)	64.41(1)	0.497(5)	0.501(3)	0.005(4)
$BaTiO_3$	Sol–gel	*P*4*mm*	4.0013(9)	4.024(1)	64.440(3)	0.485(7)	0.503(4)	0.020(9)
$BaTi_{0.85}Sn_{0.15}O_3$	Solid-phase	*P*4*mm*	4.013(1)	0.4019(2)	64.75(9)	0.487(5)	0.511(6)	0.036(4)
$BaTi_{0.85}Sn_{0.15}O_3$	Sol–gel	*P*4*mm*	4.019(1)	4.021(1)	64.98(6)	0.440(8)	0.507(7)	0.040(9)
$BaSnO_3$	Solid-phase	*Pm*3*m*	4.0109(2)	–	69.41(2)	–	–	–
$BaSnO_3$	Sol–gel	*Pm*3*m*	4.1160(3)	–	69.731(1)	–	–	–

Note: The atomic coordinates in $Ba(Ti_{1-x}Sn_x)O_3$ samples for space group *P*4*mm*: Ba, 1b (1/2 1/2 *z*); Ti/Sn, 1a (0 0 0); O(1), 1a (0 0 *z*); O(2), 2c (1/2 0 *z*) [22]; for space group *Pm*3*m*: Ba, 1b (1/2 1/2 1/2); Ti/Sn, 1a (0 0 0); O, 3d (1/2 0 0) [23].

REFERENCES

1. E. C. Subbarao, Ferroelectrics **35**, 143 (1981).
2. D. Hennings, Int. J. High Technol. Ceramics **3**, 91 (1987).
3. G. H. Jonker, Solid-State Electron. **7** (12), 895 (1964).
4. R. Vivekanandan and R. N. Kutty, Mater. Sci. Eng. **21** (7), 1190 (1990).
5. S. Halder, P. Vicror, A. Laha, et al., Solid State Commun. **121**, 329 (2002).
6. C. Kajtoch, Mat. Sci. Eng. B **64**, 25 (1999).
7. B. D. Stojanovic, A. Z. Simoes, C. O. Paiva-Santos, et al., J. Eur. Cer. Soc. **25**, 1985 (2005).
8. M. P. Pechini, US Pat. No. 3,330697 (1967).
9. C. P. Udawatte, M. Kakihana, and M. Yoshimura, Solid State Ionics **108**, 23 (1998).
10. J. Zhai, B. Shen, X. Yao, and L. Zhang, Mater. Res. Bull. **39**, 1599 (2004).
11. M. Kakihana, J. Sol-Gel Sci. Technol. **6**, 4 (1996).
12. A. Dixit, S. B. Majumder, A. Savvinov, et al., Mater. Lett. **56**, 933 (2002).
13. H. X. Zhang, C. H. Kam, Y. Chu, et al., Mat. Chem. Phys. **63**, 174 (2000).
14. D. C. Bradley, D. C. Hancock, and W. Wardlow, J. Chem. Soc., 2773 (1952).
15. D. C. Bradley, J. Chem. Soc., 4204 (1952).
16. I. Marek, *Titanium and Zirconium in Organic Synthesis* (Wiley, Weinheim, 2002), p. 512.
17. N. Yoshino, Y. Kondo, and T. Yoshino, Synth. Inorg. Met.-Org. Chem., No. 3(4), 397 (1973).
18. D. C. Bradley, E. V. Cardwell, and W. Wardlaw, J. Chem. Soc., 4775 (1957).
19. D. C. Bradley, E. V. Cardwell, and W. Wardlaw, J. Chem. Soc., 3039 (1957).
20. L. G. Sillen and A. E. Martell, *Stability Constants of Metal-Ion Complexes* (Chem. Soc, London, 1972), Spec. Publ. Nos. 17 and 25.
21. R. Drago, *Physical Methods in Chemistry* (Saunders College, Philadelphia, 1977; Mir, Moscow, 1981), Vol. 1.
22. H. T. Evans, Acta Crystallogr. **14**, 1019 (1961).
23. Y. Hinatsu, J. Solid State Chem. **122**, 384 (1996).
24. O. G. Vendik, L. T. Ter-Martirosyan, A. I. Dedyk, et al., Ferroelectrics **144**, 33 (1993).

SPELL: 1. Citratometal, 2. Polyetherification, 3. stannate, 4. frequancy